Developmental Cognitive Neuroscience 19 (2016) 98–106

Contents lists available at ScienceDirect

Developmental Cognitive Neuroscience

journal homepage: http://www.elsevier.com/locate/dcn

Spatiotemporally dissociable neural signatures for generating and updating expectation over time in children: A High Density-ERP study

Giovanni Mento[a,*], Antonino Vallesi[b,c]

[a] Department of General Psychology, University of Padova, Via Venezia, 8, 35131, Padova (PD), Italy
[b] Department of Neurosciences, University of Padova, Via Giustiniani, 5, 35128, Padova (PD), Italy
[c] Centro di Neuroscienze Cognitive, University of Padova, Italy

ARTICLE INFO

Article history:
Received 21 July 2015
Received in revised form 26 January 2016
Accepted 24 February 2016
Available online 27 February 2016

Keywords:
Temporal Orienting
Children
N1
CNV
Anticipatory Anterior Index
Brain source reconstruction

ABSTRACT

Temporal orienting (TO) is the allocation of attentional resources in time based on the *a priori* generation of temporal expectancy of relevant stimuli as well as the *a posteriori* updating of this expectancy as a function of both sensory-based evidence and elapsing time. These processes rely on dissociable cognitive mechanisms and neural networks. Yet, although there is evidence that TO may be a core mechanism for cognitive functioning in childhood, the developmental spatiotemporal neural dynamics of this mechanism are little understood. In this study we employed a combined approach based on the application of distributed source reconstruction on a high spatial resolution ERP data array obtained from eighteen 8- to 12-year-old children completing a TO paradigm in which both the cue (Temporal *vs.* Neutral) and the SOA (Short *vs.* Long) were manipulated. Results show both cue (N1) and SOA (CNV, Omission Detection Potential and Anterior Anticipatory Index) ERP effects, which were associated with expectancy generation and updating, respectively. Only cue-related effects were correlated with age, as revealed by a reduction of the N1 delta effect with increasing age. Our data suggest that the neural correlates underlying TO are already established at least from 8 to 12 years of age.

1. Introduction

The ability to anticipate 'where' and 'when' events may occur stands as a fundamental skill which allows us to selectively orient our attention in space and time (Coull and Nobre, 1998), while ignoring a myriad of other irrelevant environmental stimuli. However, while the mechanisms underlying the orienting of attention in space (*i.e.*, spatial orienting) have been thoroughly investigated in both adults (Corbetta and Shulman, 2002) and children (Amso and Scerif, 2015), the ability to orient attention in time (temporal orienting or TO) has slipped out of core attention research for many years (Nobre, 2001; Nobre and Kastner, 2014). This issue is of pivotal importance given the key role of temporal attention as a gating mechanism to select information for further computational processing, including perception, action, learning, memory and executive control (Correa, 2010).

Actually, attentional selection operates *through* time, but it is also *limited* in time, since it depends on the structural constraints imposed by the limited capacity of the human neurocognitive system. In this sense, investigating the temporal orienting of attention from a developmental cognitive neuroscience perspective may constitute a powerful heuristic for shedding light onto the temporal attention constraints and the dynamics leading to the adult end-state. Moreover, from a clinical perspective, temporal attention has been claimed to be selectively impaired in several developmental disabilities, including dyslexia (Visser, 2014), language disorders (Dispaldro et al., 2013; Dispaldro and Corradi, 2015), Attention Deficit/Hyperactivity Disorder (Carelli and Wiberg, 2012), and autism (Ronconi et al., 2013). Therefore, a better understanding of the neurocognitive underpinnings of TO as a core selective attentional mechanism in typically developing children may open new lines of research to create early, specific intervention strategies for atypical development.

The existing literature on adult individuals shows that TO can be generated by establishing temporal expectancy *a priori* according to environmentally available cues, like a temporally regular structure or a discrete signal providing predictive information about the onset of a task-relevant stimulus. In both cases, TO operates by selectively biasing attentional resources at specific points in time, resulting in faster and better behavioural performance at multiple cognitive levels (Coull and Nobre, 1998; Correa and Nobre, 2008; Correa, 2010).

* Corresponding author. Tel.: +39 0 49 827 6149; fax: +39 0 49 827 6600.
E-mail address: giovanni.mento@unipd.it (G. Mento).

http://dx.doi.org/10.1016/j.dcn.2016.02.008

Once generated, temporal expectations can be further updated *a posteriori* as a function of (1) the sensory evidence that events actually occur when expected and (2) the elapsing time itself, which intrinsically biases the distribution of attentional and motor resources over time, a phenomenon also known as the Hazard Function or HF (Niemi and Näätänen, 1981; Luce, 1986; Nobre et al., 2007; Coull, 2009a).

In a recent event-related potential (ERP) study we showed dissociable neural signatures for expectancy generation driven by discrete, informative cues and HF-related expectancy updating (Mento et al., 2015). Specifically, the first relies on a larger centro-parietal Contingent Negative Variation (CNV) showing a modulation as a function of target predictability, with the largest CNVs for the targets with the highest predictability, in line with previous literature (Capizzi et al., 2013; Mento, 2013). By contrast, HF-related expectancy updating resulted in a sustained frontal activity, showing increasing amplitude with increasing boost of subjective expectancy as a function of the passage of time. Furthermore, the source reconstruction analyses allowed identification of the origin of the CNV in a left sensorimotor cortical network, while the HF-related ERP activity was mainly generated from the lateral prefrontal cortices. Remarkably, these findings provided converging evidence with the neuroimaging literature showing distinct parietal and frontal functional networks for generating and updating temporal expectancy, respectively (Coull et al., 2000; Vallesi et al., 2009; Vallesi, 2010; Coull, 2011).

Yet, in spite of the increasing number of publications on adults, the neurocognitive mechanisms underlying TO in children are less clear. In a recent study, Johnson and collaborators (Johnson et al., 2015) employed a combined spatio-temporal cueing paradigm and found behavioural evidence that 6–16-year-old children are able to voluntarily orient their attention in space but not in time. However, as the authors argued, the lack of TO effects in their study may be due to the fact that the target was lateralized. Indeed, unlike adults (Coull and Nobre, 1998), the spatial uncertainty of target appearance may have diminished the utility of the time cue in children. In line with this account, Mento and Tarantino (2015) introduced a simplified, child-friendly TO paradigm in which the fixed central presentation of both targets together with the use of a block-wise experimental design and a fully valid CUE-SOA association allowed the demonstration of TO as early as at six years of age, suggesting that dedicated neural mechanisms are already operating at this age.

In the present study, we expanded upon these results by investigating the neural bases of TO from a developmental perspective. To this purpose, we recorded the high-density electroencephalographic (HD-EEG) activity of 8–12-year-old healthy children while administering a child-adapted TO paradigm purposely designed to investigate the neural correlates of TO generation and updating. More specifically, we assessed whether there is evidence of dissociable neural patterns for generating and updating expectation over time in children, and whether this relies on specific spatiotemporal neural signatures.

2. Materials and methods

2.1. Participants

Data were collected from eighteen healthy children [mean age: 9.3 years (SD: 2.05); range: 8–12 years; 8 males; 16 right-handed]. Since preliminary analyses did not show age-related behavioural differences, we initially considered all children as a single group and subsequently ran correlational analyses between electrophysiological components of interest and age. Visual acuity was normal or corrected to normal. All experimental methods had been previously approved by the Research Ethics Committee of the School of Psychology, University of Padua (prot. N. 1179).

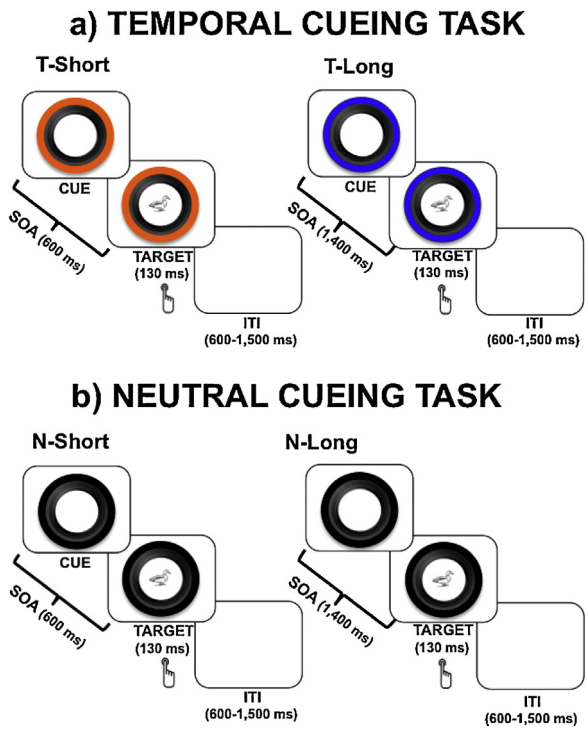

Fig. 1. Experimental paradigm. In the Temporal Cueing task (a) the visual cue provided fixed temporal information concerning the SOA duration, which could be short (left panel) or long (right panel), according to the colour of the cue. By contrast, in the Neutral Cueing task (b) participants never knew in advance the duration of the SOA, which could nevertheless have the same short or long duration as in the Temporal Cueing task.

2.2. Stimuli and task

We employed the same experimental paradigm previously used by Mento and Tarantino (2015) to investigate the behavioural correlates of temporal orienting in children (Fig. 1). Stimuli were presented on a 17-in. monitor at a resolution of 1280 × 1024 pixels. Participants were seated comfortably in a chair at a viewing distance of ~60 cm from the monitor. All participants performed two different cueing tasks within the same experimental session; these consisted of a temporal cueing task and a neutral cueing task, which were administered block-wise rather than trial-by-trial in order to reduce the top-down control required to switch continuously from a predictive to a non-predictive setting, which may result in additional difficulty for children. Importantly, the two tasks were matched for sensorimotor requirements, since the sequence of stimuli and the required responses were always the same, with the only difference between conditions being the level of temporal predictability of the target. In both tasks the trial structure was the same, as described below.

Each trial began with the display of a visual cue in the center of the screen, followed by the presentation of a target stimulus. The visual cue lasted on the screen until target onset and consisted of a picture of a black camera lens surrounded by a circle (total size of the stimulus: 840 × 840 pixels, 144 dpi, 10.62° × 10.54° of visual angle). The target stimulus consisted of a gray-scale picture of an animal, which was displayed centrally within the camera lens (840 × 840 pixels, 144 dpi, 10.62° × 10.54° of visual angle) until the response or a maximum of 3000 ms. The cue-target stimulus-onset-asynchrony (SOA) was manipulated (either 600 or 1400 ms). The Inter-Trial-Interval (ITI) was randomly and continuously

manipulated between 600 and 1500 ms. Participants were required to press the spacebar with the index finger of their dominant hand as soon as possible after the target onset. To encourage children to perform well in terms of both response speed and accuracy they were given the following instructions: "Imagine that you are at the zoo and you have a camera. Your task is to take a picture of the animals appearing within the camera lens as soon as possible. To do that, you have to press the spacebar with your index finger. Please, be careful to click as quickly as possible once you see the animals, otherwise they will disappear. Please, be also careful not to click before the animals appear!" Children were also instructed that, depending on the task, they would or would not be able to predict in advance the animals' appearance, leading to two different tasks as detailed below.

2.2.1. Temporal Cueing task

In the Temporal Cueing task (Fig. 1a), the visual cue provided fixed temporal information concerning the SOA duration. In particular, the outer circle of the camera lens was coloured either blue or orange. Each of the two colours was associated with a specific SOA duration (*i.e.*, 600 or 1400 ms) so that two task conditions were generated: a Temporal Short (T-Short) and a Temporal Long (T-Long) SOA condition. Children were explicitly told about the Cue-SOA association. In line with Mento and Tarantino (2015), the association between colours and the SOA was fixed (100% validity) and counterbalanced between subjects. No catch trials were included, that is, the target stimulus always appeared after the SOA. This was done in order to increase the likelihood of a TO effect and avoid the so-called 'dispreparation effects', as defined by (Correa et al., 2004).

2.2.2. Neutral Cueing task

In the Neutral Cueing task (Fig. 1b) the outer circle surrounding the camera lens was always black, providing no information about SOA duration. In this case the cue simply acted as a warning signal, which unspecifically prepared the participant for the upcoming target without furnishing temporal information about it. Nevertheless, as for the Temporal Cueing task, the SOA was manipulated to create a Neutral Short (N-Short) and a Neutral Long (N-Long) SOA condition (600 and 1400 ms, respectively). In line with Mento and Tarantino (2015), to maximize the hazard-ratio-related effects that induce TO updating over time, an 'aging' probability distribution (Niemi and Näätänen, 1981; Trillenberg et al., 2000) was used, with an equal a priori odds ratio (50%) for each SOA duration.

2.3. Experimental design

Both the type of CUE (Temporal *vs.* Neutral) and the SOA length (Short *vs.* Long) were manipulated and orthogonally contrasted, leading to a 2×2 factorial design. This allowed us to test for the presence of TO (*i.e.*, cue effect) for different SOA durations. More specifically, the TO in short SOA trials was calculated by comparing N-Short and T-Short trials; the TO effect in long SOA trials was calculated by comparing N-Long and T-Long trials. Moreover, the expectancy updating was revealed by the SOA effect (*i.e.*, better performance on long SOAs) and was investigated by contrasting short and long SOA conditions within the temporal (*i.e.*, T-Short *vs.* T-Long) and the neutral (*i.e.*, N-Short *vs.* N-Long) tasks. Each child underwent a total of four experimental blocks, including two Temporal Cueing and two Neutral Cueing blocks. In the Temporal Cueing blocks a total of 120 trials (60 for the T-Short and 60 for the T-Long condition) were randomly delivered. In the remaining Neutral Cueing blocks participants were given a total of 120 trials (60 for N-Short and 60 for N-Long condition), also randomly delivered. The order of the tasks was counterbalanced between subjects. E-prime 2 software (Psychology Software Tools, Pittsburgh, USA) was used to create and administer the stimuli.

2.4. EEG recordings

During the entire task, the EEG was continuously recorded and amplified using a geodesic EEG system (EGI GES-300), through a pre-cabled high-density 128-channel HydroCel Geodesic Sensor Net (HCGSN-128; Fig. 2a) and referenced to the vertex. The sampling rate was 500 Hz. The impedance for each sensor was maintained below 30 kΩ. To reduce the presence of EOG artefacts, children were instructed to limit both eye blinks and eye movements as much as possible.

2.5. Data analysis

2.5.1. Behavioural analysis

RTs to target stimuli in all experimental conditions were recorded. RTs below 150 ms or above 1500 ms were not considered. A 2×2 repeated-measures ANOVA was performed, with CUE (Temporal *vs.* Neutral) and SOA (Short *vs.* Long) as within-subject factors. Bonferroni post hoc tests were used to correct for multiple comparisons. Effect size was calculated using the partial eta square (η_p^2).

2.5.2. ERP analysis

All EEG recordings were processed offline using the MATLAB toolbox EEGLAB (Delorme and Makeig, 2004). The data were first band-pass filtered between 0.1 and 30 Hz and segmented into epochs starting 200 ms before cue onset and ending 1500 ms after it. Epochs were then visually inspected to interpolate bad channels and remove rare artefacts. Artefact-reduced data were then subjected to Independent Component Analysis (Stone, 2002). All independent components were visually inspected and those related to eye blinks or eye movements according to their morphology and scalp distribution were discarded. The remaining components were then projected back to the electrode space to obtain cleaner EEG epochs. The remaining epochs containing excessive noise or drift ($\pm 100\ \mu V$ at any electrode) were rejected. Data were then re-referenced to the average of all electrodes and the signal was aligned to the baseline by subtracting the mean signal amplitude in the pre-stimulus interval. Subject average and grand average ERPs were generated for each electrode site and experimental condition. A mean of 51.7 ± 6 (SD) epochs per condition were accepted. A four-way ANOVA with all conditions as repeated measures yielded no significant differences were found across the conditions [$F(3,51) = 2.49$; $p > 0.7$].

Given that a 128-channel recording system and a time resolution of 2 ms (500 Hz) were employed, performing a systematic comparison of all samples would result in the severe risk of false positives. Hence, a preliminary, data-driven approach was used to identify time windows of interest for further statistical comparisons. Specifically, for both short and long SOAs the Mean Global Field Power (MGFP) was calculated as the standard deviation across electrodes at a given instant in time (Lehmann and Skrandies, 1980). This procedure gives information on differences in the global amount of synchronized activity at any time-point (Michel and Murray, 2012) and as such is suitable for identifying the time windows of the ERP components consistent across trials as large deflections (Koenig and Melie-García, 2010). Once identified, the main ERP components were statistically compared in pairs of experimental conditions by performing repeated measures, two-tailed *t*-tests over an averaged 40 ms time window centered on the peak of each component and at all 128 scalp electrodes using the Mass Univariate Analysis toolbox (Groppe et al., 2011).

All conditions were orthogonally contrasted to test for the presence of ERP differences both between (T-Short *vs.* N-Short and T-Long *vs.* N-Long) and within (T-Short *vs.* T-Long and N-Short *vs.* N-Long) tasks.

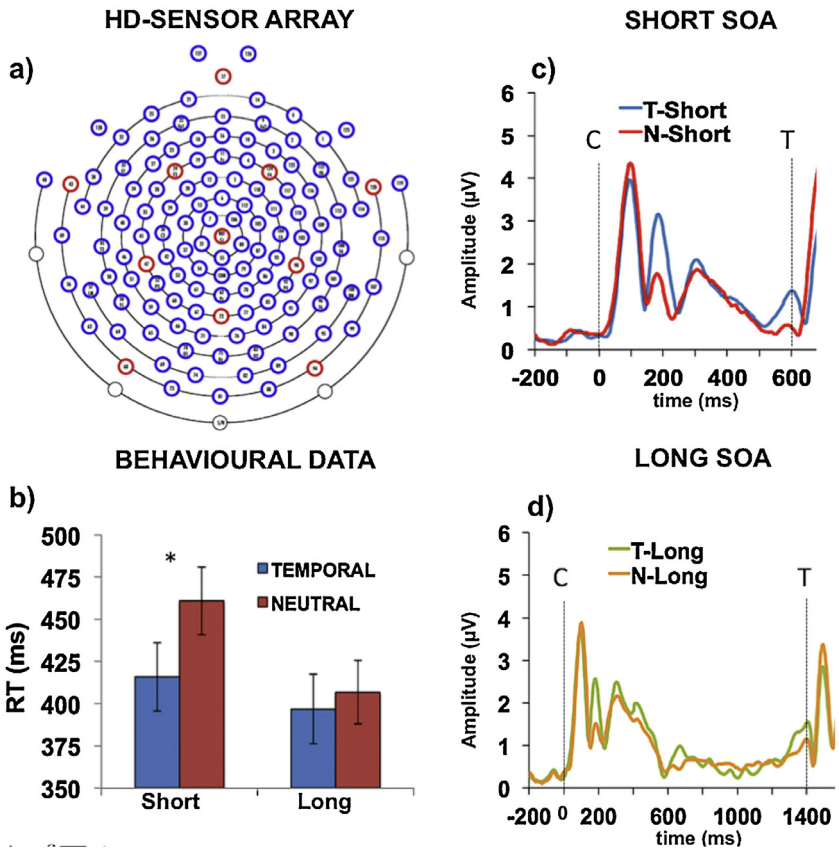

Fig. 2. (a) High-density sensor distribution over the scalp; (b) behavioural performance (RTs) of children; (c and d) show the Mean Global Field Power (MGFP) comparison of the whole scalp ERP activity (128 channels) for temporal and neutral trials at short and long SOAs, respectively. Letters C and T mark Cue and the Target onset, respectively.

The maximum amplitude peak latency of each cue-related ERP component was also measured and compared across conditions by means of a repeated-measures 2×2 ANOVA with CUE and SOA as main factors. To investigate whether TO was affected by age, both behavioural (RTs) and electrophysiological (ERP amplitude and latency) measures of each component of interest were correlated with age (in months).

2.6. Brain source reconstruction

The cortical generators underlying the ERP components of interest were reconstructed using the Brainstorm software package (Tadel et al., 2011) and adopting the same procedure as in Mento et al. (2015). The conductive head volume was modelled according to the 3-spheres BERG method (Berg and Scherg, 1994) after adjusting head radius according to age. The solution space was constrained to the cerebral cortex, which was modelled as a three-dimensional grid of 15,028 fixed dipoles oriented normally to the cortical surface. The inverse transformation was applied to the Montreal Neurological Institute (MNI) canonical mesh of the cortex to approximate real anatomy. The inverse modelling was based on a weighted minimum norm (wMN) solution implemented as a routine of the Brainstorm platform. In line with previous studies on children's cortical source reconstruction (Astle et al., 2015), for each participant the sources were projected to a standard anatomical template (MNI) and their activity was transformed in absolute Z scores relative to the baseline. The cortical activations were located according to the anatomical Desikan–Killany atlas (Desikan et al., 2006) adapted for cortical space solution. Brodmann areas (BA) associated with the stereotaxic coordinates and maxima MNI coordinates of cortical regions of interest (ROI) were also reported.

3. Results

3.1. Behavioural results

Performance in this task reached a high accuracy level ($93.75 \pm 0.87\%$ correct) and was not different between conditions ($p > 0.5$). The behavioural benefits conferred by TO were observed mainly in reaction times (RTs). As shown in Fig. 2b, children were overall faster not only when targets were temporally predictable (main effect of the CUE; $F(1,17) = 5.66$; $p < .03$; $\eta_p^2 = 0.25$) but also when the latter were preceded by long rather than short SOAs (main effect of the SOA; $F(1,17) = 18.83$; $p < 0.0001$; $\eta_p^2 = 0.53$). In addition, a significant CUE $\times$ SOA interaction ($F(1,17) = 6.03$; $p < 0.03$; $\eta_p^2 = 0.26$) revealed that TO produced an asymmetrical effect, as the speeding up of RTs induced by the temporal cue was present for short ($p < 0.01$) but not long ($p > 0.4$) SOAs.

3.2. ERP results

3.2.1. Cue-related ERP activity

The inspection of the MGFP activity showed a consistent morphological pattern for both short (Fig. 2c) and long (Fig. 2d) SOA cue-related ERP activity. This included a first component peaking at about 100 ms after cue onset (P1) followed by a second peak at about 200 ms (N1) and by a third peak at about 300 ms (P2). At a false discovery rate of 0.05, the adjusted alpha (B-Y critical p) for all comparison time windows was 0.0038 corresponding to a critical t-score of ± 3.32, which means that all observed t-values exceeding the critical score were considered significant. The statistics only revealed a significant between-task modulation of the N1 component, which was larger in the temporal than in the neutral task

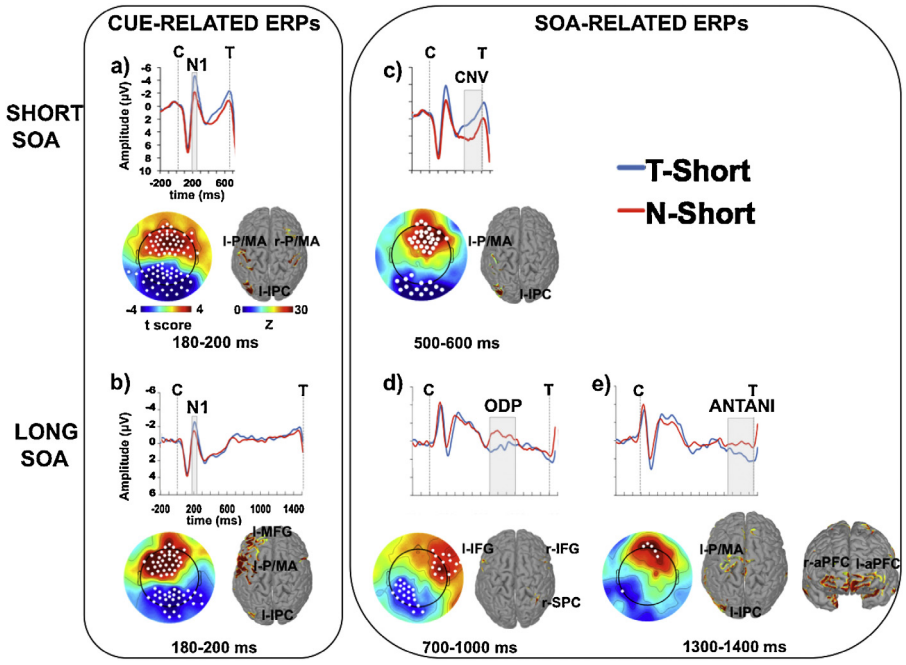

Fig. 3. HD-ERP activity. Each plot displays the HD-ERP activity averaged across electrodes exceeding the critical *t*-score threshold for statistical significance ($_{\text{FDR-corrected}}$ $p < 0.05$). These are shown below the waveform plots as white dots on the *t*-score scalp maps. The cortical source reconstruction relative to each significant effect is also shown alongside. Source activations are plotted as *Z* scores and are adjusted using a threshold of 50% of the maximum amplitude and a size of at least 10 vertices. The left panel shows the cue-related ERP effects. These include a N1 modulatory effect for both the short (a) and the long (b) SOA condition. The right panel shows the SOA-related effects entailing the CNV elicited in short SOA conditions (c) and reflecting expectancy implementation as well as the Omission Detection Potential (ODP; d) and the Anterior Anticipatory Index (ANTANI; e) in long SOA conditions, reflecting sensory- and Hazard Function-based temporal expectancy updating, respectively.

for both short (Fig. 3a) and long (Fig. 3b) SOAs. Moreover, the N1 showed a further within-task modulation since it was larger for the T-Short than the T-Long condition. As expected, no N1 differences were found within the neutral task, as in this case the cue was not manipulated. No significant latency effects were found (all $Fs < 2$; all $ps > 0.2$). The brain source reconstruction revealed that the N1 effect at short SOAs was supported by the activation of a sensorimotor network including the left inferior parietal lobule (BA 40; peak $x = -37$, $y = -59$, $z = 45$), and the left (BA 4; peak $x = -49$, $y = -11$, $z = 52$) and right (BA 4; peak $x = 52$, $y = -15$, $z = 51$) pre-central gyri. Concerning the long SOAs, the N1 effect was supported by the activation of the left inferior parietal cortex (BA 40; peak $x = -30$, $y = -76$, $z = 33$), the left pre-central gyrus (BA 4; peak $x = -39$, $y = -13$, $z = 49$) and the left middle frontal gyrus (l-MFG; BA 46; peak $x = -43$, $y = -48$, $z = 21$).

3.2.2. SOA-related ERP activity

In addition to the early N1 effect, the MGFP calculated on short SOA trials (Fig. 2c) showed a later component occurring about 100 ms before target onset. The statistics confirmed that this component was significantly larger for temporal than neutral trials (Fig. 3c), compatible with a CNV-like response. However, while in adult TO tasks the CNV has been described as a wide centro-parietal CNV (Miniussi et al., 1999; Capizzi et al., 2013; Mento et al., 2013, 2015), the topographical maps showed that in children this was expressed as a posterior negative/anterior positive dipolar configuration. Similarly to the N1, the cortical generators of the CNV included the left inferior parietal cortex (BA 40; peak $x = -40$, $y = -61$, $z = 48$) and the left pre-central gyrus (BA 4 peak $x = -43$, $y = -13$, $z = 57$).

Concerning long trials, the MGFP (Fig. 2d) allowed the identification of two distinct SOA-related components. The first one consisted of a middle latency ERP between about 700 and 1000 ms and was characterized by significantly larger amplitudes for neutral than temporal trials ($t > \pm 3.32$; $_{\text{B-Y FDR corrected}}$ $p < 0.05$), as shown in Fig. 3d. As a possible explanation for this effect, we speculated that the omission of the target at the short SOA in N-Long trials may have yielded an expectancy updating due to the sensory evidence that the target did not appear at the first useful interval. This is in line with similar effects elicited by the absence of an expected auditory (Todorovic et al., 2011; Wacongne et al., 2012) or visual (Ng and Penney, 2014) stimulus. Given that previous studies did not provide a common definition for this effect, here we defined it as the Omission Detection Potential (ODP). This effect was located bilaterally in the inferior frontal gyrus (BA 9; peak $x = -60$, $y = 13$, $z = 31$ and $x = 57$, $y = 11$, $z = 31$) and in the right superior parietal lobule (BA 40; peak $x = 51$, $y = -51$, $z = 31$).

The second SOA-related ERP component occurred between about 1100 and 1400 ms after cue onset and was significantly larger for the temporal than neutral condition ($t > \pm 3.32$; $_{\text{B-Y FDR corrected}}$ $p < 0.05$). Yet, as shown in Fig. 3e, the scalp map revealed a different topographical distribution since in this case the effect was mainly focused on the anterior electrodes, suggesting that this signature may reflect a different process according to SOA length. Hence, to distinguish it from the CNV elicited at the short SOA, we decided to name this component the Anterior Anticipatory Index (ANTANI). The ANTANI effect involved a left sensorimotor network including inferior parietal cortex (BA 40; peak $x = -57$, $y = -49$, $z = 40$) and left pre-central gyrus (BA 4; peak $x = -40$, $y = -15$, $z = 51$) together with an additional bilateral recruitment of the anterior portion of the superior and middle frontal gyri (BA 10/46; peak $x = 22$, $y = 67$, $z = -6$ and B10/46; peak $x = 25$, $y = 65$, $z = -1$ for the left and right lobe respectively), here commonly identified as the left and the right anterior prefrontal cortex (r- and l-aPFC).

To better describe the spatiotemporal dynamics of the neural generators underlying the ERP effects, the activation time course was extracted at regions of interest (ROIs) visually identified in the cortical maps and compared between short and long SOA conditions (Fig. 4). Globally, this comparison provided additional

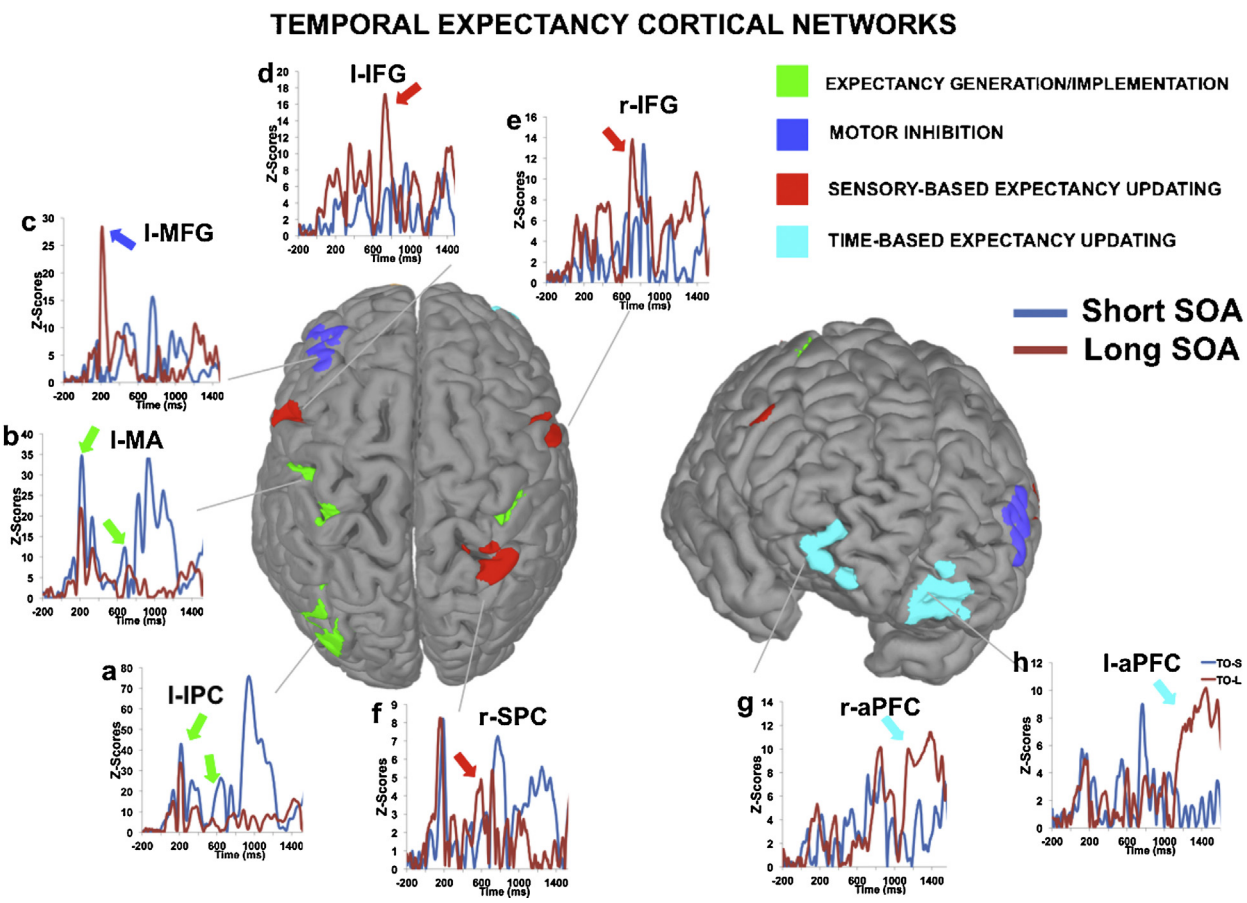

Fig. 4. Neural networks underlying expectations generation and updating. The central part of the figure shows a summary of the major cortical ROIs underlying the scalp-related significant ERP effects. The different colours identify spatiotemporally dissociable neural networks involved in distinct computational stages underlying temporal expectation and updating. Each panel shows the comparison of the time course of single cortical areas between short and long SOAs. Coloured arrows indicate the peak of activity for each cortical ROI.

evidence supporting the existence of distinct cortical networks involved in different TO processing stages. In particular, the l-IPC (Fig. 4a) and the premotor/motor (P/MA) areas (Fig. 4b) displayed a first transient peak of activity between 180 and 200 ms, corresponding to the N1 temporal range. This finding suggests the engagement of a first sensorimotor network in the *a priori* generation of temporal expectation on the basis of learned cue-SOA associations. Furthermore, in the same temporal window, we identified an additional and transient activation of the l-MFG (Fig. 4c), but only for long SOA trials. A second spatiotemporal cortical pattern was identified at a later temporal window, peaking in the range of the ODP response (*i.e.*, between 600 and 800 ms). This circuit was exclusively detected following T-Long cues and involved both the left (Fig. 4d) and the right (Fig. 4e) IFG as well as the right SPC (Fig. 4f). Finally, a third spatiotemporal pattern of cortical activity was detected. This included the anterior bilateral portion of the prefrontal cortices (Fig. 4g and h), which displayed a progressive activation a few hundreds of milliseconds before target onset and peaked in correspondence to it.

3.3. Correlational analyses

As expected, Pearson's correlations revealed that RTs were negatively correlated with age for all conditions (all $r_s > -0.55$; all $p_s < 0.02$). However, when looking at the Cue and SOA effects derived by both between- and within-task pair-wise comparisons, we did not find significant correlations with age. That is, although the behavioural performance (*i.e.*, RT speed) globally improved with age, the ability to generate and update temporal expectation was stable from 8 to 12 years of age. This result is consistent with our previous findings showing that both the TO induced by cues (Mento and Tarantino, 2015) and the foreperiod effect related to SOA manipulation (Vallesi and Shallice, 2007) are already established and quite stable from 8 years of age onward.

Moreover, we correlated age with the amplitude and the latency of the averaged ERP activity on each s-ROI obtained by clustering the adjacent electrodes that showed significant effects for each statistical comparison. These analyses yielded significant correlations between age and the amplitude of the N1 at the posterior s-ROI for the temporal ($r = 0.55$; $p < 0.02$ for T-Short and $r = 0.49$; $p < 0.05$ for T-Long) but not the neutral (all $r_s < 0.17$; all $p_s > 0.33$) conditions. We also found that age was significantly correlated with the amplitude of both the CNV and the ANTANI components at the posterior s-ROI for both the temporal and neutral conditions (all $r_s > 0.48$; all $p_s < 0.05$). That is, the ANTANI amplitude was globally larger as age increased, in line with what was observed for the N1. Likewise, we found a positive correlation between age and the amplitude of the ODP measured at both the anterior and posterior s-ROIs (all $r_s > .46$; all $p_s < 0.05$). Concerning the TO effects measured by contrasting ERP amplitudes between temporal and neutral trials at both SOAs, we found a significant correlation between age and the N1 modulation (delta N1) for both short ($r = 0.66$; $p < 0.01$) and long ($r = 0.56$; $p < 0.02$) trials. Specifically, as shown in Fig. 5, the delta N1 was larger at younger ages and tended to disappear as age increased. By contrast, no significant correlations emerged between age and SOA-related ERPs.

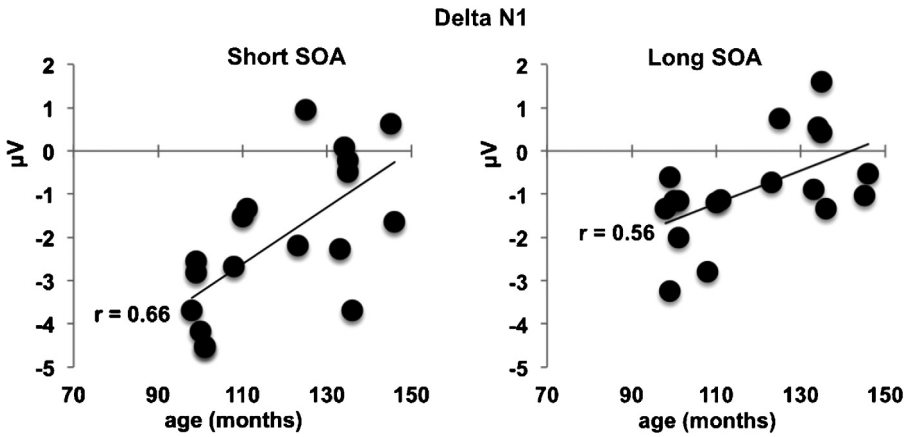

Fig. 5. Correlation between age and ERP effects. Graphs show the distribution of the N1 delta effect obtained by subtracting the N1 amplitude in neutral trials from the one measured in temporal trials as a function of age as well as the regression line for short (left panel) and long (right panel) SOAs.

4. Discussion

In this High Density-ERP study, we investigated both the behavioural correlates and the spatiotemporal neural signatures of temporal expectancy induced by discrete, informative cues in 8–12 year-old children. The behavioural results showed faster motor responses to temporally than neutrally cued targets at short SOAs but not at long ones. This finding is consistent with our previous study (Mento and Tarantino, 2015) in suggesting that 8–12 year-old children can successfully generate and implement *a priori* temporal expectations based on the information provided by discrete cues.

Importantly, the absence of TO effects together with the overall RT speeding up at long SOAs further confirmed that children are able to update such expectations *a posteriori*, in line with Vallesi and Shallice (2007). In contrast with our results, a recent study by Johnson et al. (2015) failed to find evidence of TO in 6–16-year-old children. However, Johnson and colleagues used a mixed spatial-temporal paradigm with lateralized stimuli and also introduced an invalid cue condition, which could have made the task considerably more difficult for young children. To overcome this possible shortcoming, in the present study we adopted a very simple, child-friendly experimental protocol characterized by a block-wise experimental design and by a fully valid cue informativeness. This may have made it easier for children to succeed in the task, and to produce robust TO behavioural effects.

In line with the behavioural data, the ERP findings provided evidence of dissociable spatiotemporal neural signatures reflecting discrete TO computational stages in children. Specifically, we found that the early ERP activity was modulated by the symbolic value of the cue, reflecting expectancy generation. By contrast, the late ERP activity reflected the updating of expectancy induced by the SOA duration itself, as described below.

4.1. Neural signatures of expectancy generation

The ERP signatures of expectancy generation consisted of a modulation of the cue-related N1, which was larger following temporal than neutral cues regardless of the predicted interval (short or long). Noticeably, since the symbolic value of the cue (the colour-SOA association) was counterbalanced across participants, we can exclude the possibility that this effect reflects differences in low-level perceptual cue feature processing, including the colour, the luminance or the contrast of the stimuli. This account is further supported by evidence that (1) the earlier P1 was never affected by cue manipulation and (2) the N1 was further modulated within-task according to the specific temporal information conveyed by the cue, in that it was larger following temporal short cues compared to temporal long cues. These considerations suggest that children are able to endogenously generate temporal expectancy resulting in the allocation of more resources to temporal cues than neutral ones, and to temporal short cues than temporal long ones.

Thus, the N1 modulatory effect may reliably reflect cue-related temporal expectancy generation. Remarkably, the N1 amplitude modulation between temporal and neutral cues (delta N1) showed a significant decrease as a function of age. This may suggest that the endogenous generation of temporal expectancy is more demanding for younger children. In fact, in order to successfully generate temporal expectancy on the basis of discrete cues and consequently allocate attentional/motor resources after short or long intervals, children are required to encode, maintain and retrieve from memory the learned Cue-SOA association as well as to switch continuously from short to long SOAs and vice versa. It is reasonable to suppose that all these processes may be more effortful for younger as compared to older children, even in our restricted age-range. As a further confirmation of this hypothesis, in a previous study investigating the neural correlates of TO with a similar paradigm in adults (Mento et al., 2015), we did not observe the N1 modulation reported here.

Additional ERP modulations were also found at a later time window reflecting SOA-related activity and including both the implementation and the updating of prior established expectations. Specifically, in TO tasks the implementation phase can be conceived of as relying on feedforward enhanced motor preparation in the specific intervals in which targets are predicted to occur according to prior generated expectation (Coull, 2011). Importantly, the implementation component is involved regardless of the SOA, since in all cases participants are allowed to prepare for specific points in time. While in adults the main ERP hallmark of this process has been identified as the CNV component (Miniussi et al., 1999; Kononowicz and van Rijn, 2011, 2014; Los and Heslenfeld, 2005; Capizzi et al., 2013; Mento et al., 2013, 2015), we observed in children a morphologically different pattern, characterized by an anterior/posterior dipolar activity arising about 100 ms before the onset of predictable targets. Although the functional role of this component in children is not entirely clear, the fact that it displayed the same modulation as the one observed for the CNV in adults in similar paradigms (*i.e.*, larger amplitudes preceding predictable targets with short SOA *vs.* unpredictable targets), together with the evidence of faster behavioural performance following larger CNVs, led us to suppose that it can reflect a similar functional mechanism as that described in adults (*e.g.*, Capizzi et al., 2013; Los and Heslenfeld, 2005; Mento et al., 2015; Miniussi et al., 1999).

For this reason we used the same definition as that used in the adult literature. Previous neuroimaging studies on adults suggested a key role of left sensorimotor network for the *feedforward* generation/implementation of temporal expectations (Coull, 2010, 2011). Consistent with this account, brain source reconstruction identified a clear-cut cortical pattern including the left inferior parietal (l-IPC) and the precentral gyrus around motor/premotor (P/MA) areas underlying both the N1 and the CNV components. Crucially, the activation time-course of these cortical ROIs further showed that this left sensorimotor circuit showed a double peak of activity, that is, at about 200 ms after cue onset (N1 range) and at about one hundred milliseconds before target onset (CNV range). This finding may suggest that a unique neural network recruited for *a priori* temporal expectation generation (and expressed at the scalp in the N1 temporal range) may be subsequently engaged in the implementation of this expectation over time, a process expressed at the scalp level by the CNV component in children similarly to what was found in adults (Mento et al., 2015).

Noteworthy, as a limitation of the present study, it has to be recognized that the expectancy generation and implementation phases cannot be completely dissociated within the experimental paradigm we used, since all TO contrasts included both these processes. However, in support of the account that the N1 and the CNV components reflect dissociable processes, we found that while the delta N1 effect vanished as age increased, no correlations between age and the delta CNV effect emerged. This dissociation can be explained by assuming that only the time expectancy generation phase is affected by development (at least for the age-range investigated here), since it requires much more cognitive effort than that needed for the implementation following a previously generated temporal expectancy, which simply relies on the translation of the previously generated expectation into a motor preparation enhancement.

In addition to the left sensorimotor network detected for the N1/CNV effects, a left prefrontal activity mainly involving the l-MFG was found. Unlike the parietal and motor/premotor areas, this region showed a single peak of activity in the N1 range and only for long SOAs. This finding may be explained by assuming that when a long expectation is predicted there is an additional recruitment of an inhibitory process, since in this case participants must strategically postpone motor preparation to later points in time (Mento et al., 2015). This hypothesis is further corroborated by data showing a key role of the middle frontal gyrus in inhibitory go/nogo tasks in adult (Song and Hakoda, 2015) and developmental (Heitzeg et al., 2014; Vara et al., 2014) populations.

4.2. Neural signatures of Expectancy Updating

The duration of the cue-target interval determines the need of participants to update their prior expectation, given that the conditional probability of target occurrence is, by definition, biased by the passage of time (Niemi and Näätänen, 1981; Luce, 1986; Nobre et al., 2007; Coull, 2009b; Vallesi, 2010). Accordingly, in long SOA trials children must integrate their prior expectancy with the sensory evidence about the actual occurrence of events at the expected time. Additionally, they must internally make use of the passage of time, which in itself induces a boost of expectancy that the event will occur at the next time since it has not yet occurred (*e.g.*, Niemi and Näätänen, 1981; Trillenberg et al., 2000).

The expectancy updating was revealed in our data by the presence of a double ERP signature elicited in long SOA trials only. The first consisted of the elicitation of an Omission Detection Potential (ODP) peaking between 700 and 1000 ms after cue onset, that is, a few hundred ms from the end of the first probable interval of target occurrence in neutral trials. A larger ODP for neutral than temporal long trials may reasonably reflect the sensory-based expectancy updating mechanism prompted by the evidence that the target has not appeared at the short SOA interval. Specifically, the ODP could mark the detection of the end of the short SOA, after which a preparatory process that was previously held in stand-by mode would begin. In fact, when the target is not presented at the short SOA in the neutral task, children realize that it will inescapably occur at the long SOA. In other words, children could use the evidence of target omission at the short SOA as the anchor point to start response preparation for the longer interval. This preparatory process may be related to the HF-related expectancy updating and would rely on the larger frontal ERP activity for temporal as compared to neutral trials, an effect that we defined as the Anterior Anticipatory Index or ANTANI. This ERP signature may reflect the recruitment of additional cognitive resources dealing with the HF-related expectancy updating. In other words, besides implementing the *a priori* established expectancy according to the cue, children further need to *a posteriori* update such knowledge over time. In line with this account the absence of significant posterior effects is compatible with the fact that at long SOAs both temporal and neutral conditions are equally predictable, and is also confirmed by the absence of significant behavioural differences. Hence, no substantial CNV modulatory effects are elicited. At the same time, the significant frontal difference found in long SOA trials, here defined as ANTANI, may reflect the HF-related increase of subjective temporal expectancy of target occurrence due to its temporal certainty.

The cortical sources of SOA-related ERPs at long SOAs included two temporally distinct networks. In particular, the sensory-based expectancy updating marked by the ODP mainly involved a front-parietal network including the inferior frontal gyrus bilaterally together with the right superior parietal cortex. By contrast, the ANTANI effect was underpinned by a bilateral recruitment of the anterior prefrontal cortices (including the rostral portion of both superior and medial frontal gyri) in addition to the same left sensorimotor network identified at short SOAs. In other words, compared to short SOA trials, the long SOA trials implicated the recruitment of a broader network including both cortical regions underlying *a priori* expectation implementation and *a posteriori* HF-related expectation updating, compatible with previous neuroimaging evidence on adults (Coull et al., 2000; Mento et al., 2015; Vallesi et al., 2007, 2009; Vallesi, 2010).

5. Limitations and conclusions

The present study provides the first evidence that children can generate, implement and update temporal expectations resulting in distinct spatiotemporal electrophysiological signatures mostly comparable with similar phenomena observed in adults (Mento et al., 2015). These include specific ERP modulatory effects elicited by both the cue symbolic value (temporal *vs.* neutral) and by the length of the SOA (short *vs.* long). Brain source reconstruction provided further evidence for spatiotemporally dissociable cortical networks underlying each single computational stage described above. Yet, the interpretation of source reconstruction findings requires caution due to the low spatial resolution of EEG as well as to the fact that we did not have single-subject head models or three-dimensional coordinates of the actual electrode positions, which would have improved the accuracy of cortical source localization. Therefore, future studies based on higher spatial resolution techniques, like fMRI or fNIRS, are needed to further corroborate our findings. Notwithstanding this methodological caveat, it is important to outline that the neural networks we identified are consistent with those found in previous neuroimaging studies on adults (Cotti et al., 2011; Coull and Nobre, 1998; Coull et al., 2000; Coull, 2009a, 2011; Mento et al., 2015; Vallesi et al., 2007, 2009; Wiener et al., 2010).

To conclude, the present study contributes to the current knowledge of the neuro-developmental basis of temporal orienting as a core selective attentional mechanism, suggesting that both the cognitive mechanisms and the corresponding neural circuitry are only partially different in children and adults.

Conflict of interest

The authors declare no competing financial interests.

Acknowledgements

The authors kindly thank Dr. Pietro Scatturin for laboratory technical support and Dr. Laura Babcock for English manuscript proof-reading. A special thank goes also to all children and their families for participating to the study. This work was supported by the grant "Progetto Giovani Studiosi" from the University of Padua (Prot. 1682/2012) to G. M. and by the FP7/2007-2013 European Research Council Starting grant LEX-MEA to A. V. (GA# 313692).

References

Amso, D., Scerif, G., 2015. The attentive brain: insights from developmental cognitive neuroscience. Nat. Rev. 16, 606–619.
Astle, D.E., Luckhoo, H., Woolrich, M., Kuo, B.-C., Nobre, A.C., Scerif, G., 2015. The neural dynamics of fronto-parietal networks in childhood revealed using magnetoencephalography. Cereb. Cortex 25, 3868–3876.
Berg, P., Scherg, M., 1994. A fast method for forward computation of multiple-shell spherical head models. Electroencephalogr. Clin. Neurophysiol. 90, 58–64.
Capizzi, M., Correa, A., Sanabria, D., 2013. Temporal orienting of attention is interfered by concurrent working memory updating. Neuropsychologia 51, 326–339.
Carelli, M.G., Wiberg, B., 2012. Time out of mind: temporal perspective in adults with ADHD. J. Atten. Disord. 16, 460–466.
Corbetta, M., Shulman, G.L., 2002. Control of goal-directed and stimulus-driven attention in the brain. Nat. Rev. Neurosci. 3, 201–215.
Correa, A., 2010. Enhancing behavioural performance by visual temporal orienting. In: Coull, J., Nobre, A. (Eds.), Attention and Time. Oxford University Press, Oxford, pp. 359–370.
Correa, Á., Lupiáñez, J., Milliken, B., Tudela, P., 2004. Endogenous temporal orienting of attention in detection and discrimination tasks. Percept. Psychophys. 66, 264–278.
Correa, A., Nobre, A.C., 2008. Neural modulation by regularity and passage of time. J. Neurophysiol. 100, 1649–1655.
Cotti, J., Rohenkohl, G., Stokes, M., Nobre, A.C., Coull, J.T., 2011. Functionally dissociating temporal and motor components of response preparation in left intraparietal sulcus. Neuroimage 54, 1221–1230.
Coull, J., 2009a. Neural substrates of mounting temporal expectation. PLoS Biol. 7, e1000166.
Coull, J., 2010. Neural substrates of temporal attentional orienting – Oxford Scholarship. In: Nobre, A., Coull, J. (Eds.), Attention to Time. Oxford University Press.
Coull, J.T., 2011. Discrete neuroanatomical substrates for generating and updating temporal expectations. In: Space Time Number Brain., pp. 87–101.
Coull, J.T., Frith, C.D., Büchel, C., Nobre, A.C., Bu, C., Nobre, A.C., 2000. Orienting attention in time: behavioural and neuroanatomical distinction between exogenous and endogenous shifts. Neuropsychologia 38, 808–819.
Coull, J.T., Nobre, A.C., 1998. Where and when to pay attention: the neural systems for directing attention to spatial locations and to time intervals as revealed by both PET and fMRI. J. Neurosci. 18, 7426–7435.
Coull, J.T.J., 2009b. Neural substrates of mounting temporal expectation. PLoS Biol. 7, e1000166.
Delorme, A., Makeig, S., 2004. EEGLAB: an open source toolbox for analysis of single-trial EEG dynamics including independent component analysis. J. Neurosci. Methods 134, 9–21.
Desikan, R.S., Ségonne, F., Fischl, B., Quinn, B.T., Dickerson, B.C., Blacker, D., Buckner, R.L., Dale, A.M., Maguire, R.P., Hyman, B.T., Albert, M.S., Killiany, R.J., 2006. An automated labeling system for subdividing the human cerebral cortex on MRI scans into gyral based regions of interest. Neuroimage 31, 968–980.
Dispaldro, M., Corradi, N., 2015. The effect of spatio-temporal distance between visual stimuli on information processing in children with Specific Language Impairment. Res. Dev. Disabil. 45–46, 284–299.
Dispaldro, M., Leonard, L.B., Corradi, N., Ruffino, M., Bronte, T., Facoetti, A., 2013. Visual attentional engagement deficits in children with Specific Language Impairment and their role in real-time language processing. Cortex 49, 2126–2139.
Groppe, D.M., Urbach, T.P., Kutas, M., 2011. Mass univariate analysis of event-related brain potentials/fields I: a critical tutorial review. Psychophysiology 48, 1711–1725.
Heitzeg, M.M., Nigg, J.T., Hardee, J.E., Soules, M., Steinberg, D., Zubieta, J.-K., Zucker, R.A., 2014. Left middle frontal gyrus response to inhibitory errors in children prospectively predicts early problem substance use. Drug Alcohol Depend. 141, 51–57.
Johnson, K.A., Burrowes, E., Coull, J.T., 2015. Children can implicitly, but not voluntarily, direct attention in time. PLoS ONE 10, e0123625.
Koenig, T., Melie-García, L., 2010. A method to determine the presence of averaged event-related fields using randomization tests. Brain Topogr. 23, 233–242.
Kononowicz, T.W., van Rijn, H., 2011. Slow potentials in time estimation: the role of temporal accumulation and habituation. Front. Integr. Neurosci. 5, 48.
Kononowicz, T.W., van Rijn, H., 2014. Decoupling interval timing and climbing neural activity: a dissociation between CNV and N1P2 amplitudes. J. Neurosci. 34, 2931–2939.
Lehmann, D., Skrandies, W., 1980. Reference-free identification of components of checkerboard-evoked multichannel potential fields. Electroencephalogr. Clin. Neurophysiol. 48, 609–621.
Los, S.a., Heslenfeld, D.J., 2005. Intentional and unintentional contributions to nonspecific preparation: electrophysiological evidence. J. Exp. Psychol. Gen. 134, 52–72.
Luce, R.D., 1986. Response Times: Their Role in Inferring Elementary Mental Organization. University Press, New York.
Mento, G., 2013. The passive CNV: carving out the contribution of task-related processes to expectancy. Front. Hum. Neurosci. 7, 827.
Mento, G., Tarantino, V., 2015. Developmental trajectories of internally and externally driven temporal prediction. PLoS ONE 10, e0135098.
Mento, G., Tarantino, V., Sarlo, M., Bisiacchi, P.S., 2013. Automatic temporal expectancy: a high-density event-related potential study. PLoS ONE 8, e62896.
Mento, G., Tarantino, V., Vallesi, A., Bisiacchi, P.S., 2015. Spatiotemporal neurodynamics underlying internally and externally driven temporal prediction: a high spatial resolution ERP study. J. Cogn. Neurosci. 27, 425–439.
Michel, C.M., Murray, M.M., 2012. Towards the utilization of EEG as a brain imaging tool. Neuroimage 61, 371–385.
Miniussi, C., Wilding, E.L., Coull, J.T., Nobre, a.C., 1999. Orienting attention in time. Modulation of brain potentials. Brain 122 (Pt 8), 1507–1518.
Ng, K.K., Penney, T.B., 2014. Probing interval timing with scalp-recorded electroencephalography (EEG). Adv. Exp. Med. Biol. 829, 187–207.
Niemi, P., Näätänen, R., 1981. Foreperiod and simple reaction time. Psychol. Bull. 89, 133–162.
Nobre, a.C., 2001. The attentive homunculus: now you see it, now you don't. Neurosci. Biobehav. Rev. 25, 477–496.
Nobre, A., Correa, A., Coull, J., 2007. The hazards of time. Curr. Opin. Neurobiol. 17, 465–470.
Nobre, A., Kastner, S., 2014. In: Nobre, A., Kastner, S. (Eds.), The Oxford Handbook of Attention.
Ronconi, L., Gori, S., Giora, E., Ruffino, M., Molteni, M., Facoetti, A., 2013. Brain and Cognition Deeper attentional masking by lateral objects in children with autism. Brain Cogn. 82, 213–218.
Song, Y., Hakoda, Y., 2015. An fMRI study of the functional mechanisms of Stroop/reverse-Stroop effects. Behav. Brain Res. 290, 187–196.
Stone, J.V., 2002. Independent component analysis: an introduction. Trends Cogn. Sci. 6, 59–64.
Tadel, F., Baillet, S., Mosher, J.C., Pantazis, D., Leahy, R.M., 2011. Brainstorm: a user-friendly application for MEG/EEG analysis. Comput. Intell. Neurosci., 879716.
Todorovic, A., van Ede, F., Maris, E., de Lange, F.P., 2011. Prior expectation mediates neural adaptation to repeated sounds in the auditory cortex: an MEG study. J. Neurosci. 31, 9118–9123.
Trillenberg, P., Verleger, R., Wascher, E., Wauschkuhn, B., Wessel, K., 2000. CNV and temporal uncertainty with 'ageing' and 'non-ageing' S1–S2 intervals. Clin. Neurophysiol. 111, 1216–1226.
Vallesi, A., 2010. Neuro-anatomical substrates of foreperiod effects. In: Coull, J.T., Nobre, A.C. (Eds.), Attention and Time. Oxford University Press, Oxford, pp. 303–316.
Vallesi, A., McIntosh, A.R., Shallice, T., Stuss, D.T., 2009. When time shapes behavior: fMRI evidence of brain correlates of temporal monitoring. J. Cogn. Neurosci. 21, 1116–1126.
Vallesi, A., Shallice, T., 2007. Developmental dissociations of preparation over time: deconstructing the variable foreperiod phenomena. J. Exp. Psychol. Hum. Percept. Perform. 33, 1377–1388.
Vallesi, A., Shallice, T., Walsh, V., 2007. Role of the prefrontal cortex in the foreperiod effect: TMS evidence for dual mechanisms in temporal preparation. Cereb. Cortex 17, 466–474.
Vara, A.S., Pang, E.W., Vidal, J., Anagnostou, E., Taylor, M.J., 2014. Neural mechanisms of inhibitory control continue to mature in adolescence. Dev. Cogn. Neurosci. 10, 129–139.
Visser, T.A.W., 2014. Evidence for deficits in the temporal attention span of poor readers. PLoS ONE 9, e91278.
Wacongne, C., Changeux, J.-P., Dehaene, S., 2012. A neuronal model of predictive coding accounting for the mismatch negativity. J. Neurosci. 32, 3665–3678.
Wiener, M., Turkeltaub, P., Coslett, H., 2010. implicit timing activates the left inferior parietal cortex. Neuropsychologia 48, 3967–3971.